Appl. Phys. 3, 37—43 (1974)

Applied Physics

Equilibrium Vacancy Concentration Measurements on Aluminum

B. von Guérard*, H. Peisl*, and R. Zitzmann
I. Physikalisches Institut, Technische Hochschule, D-6100 Darmstadt, Fed. Rep. Germany

Received 20 September 1973

Abstract. Thermal expansion on high purity aluminum has been measured to study defects in thermal equilibrium by the $(\Delta L/L_0 - \Delta a/a_0)$ method. Measurements of the changes in macroscopic length ΔL and lattice parameter Δa were made from room temperature to 637° C. Length changes were measured by a laser interferometer and lattice parameter changes by a X-ray diffractometer technique on the same crystal at identical temperatures. At temperatures above 400° C $\Delta L/L_0$ becomes greater than $\Delta a/a_0$, indicating the generation of a noticeable amount of new lattice sites due to vacancy formation. Extrapolation gives a vacancy concentration $\Delta N/N_0 = 9.8 \cdot 10^{-4}$ at the melting point (660° C). The experimental findings can be explained by assuming formation of monovacancies and divacancies. Values for the enthalpy and entropy of formation for mono- and divacancies are given.

Index Headings: Thermal expansion measurements – Equilibrium vacancy concentration in aluminum

The study of point defects in thermal equilibrium has been the subject of a great number of investigations in the past [1–3]. It has been commonly accepted that in the case of vacancy type defects the best method for obtaining absolute values of the equilibrium defect concentration close to the melting point is the $(\Delta L/L_0 - \Delta a/a_0)$ method [4, 5]. This method compares the macroscopic thermal expansion $\Delta L/L_0$ with the thermal expansion of the lattice parameter $\Delta a/a_0$ as measured by X-ray diffraction. Several authors have investigated vacancy formation in the fcc metal aluminum by this method [4–6]. Seperation of the contributions due to mono- and divacancies, respectively, to the results is difficult. Further progress in positron annihilation studies [7] of point defects in thermal equilibrium gives rather unambiguous results for the monovacancy formation energy. Thus the $(\Delta L/L_0 - \Delta a/a_0)$ method can be used to determine the contribution of divacancies.

* New address: Physik-Department, Technische Universität München, D-8046 Garching, Fed. Rep. Germany.

In Section 1, we scetch the principles of the method. In Section 2 the experiment is described in some detail. Section 3 gives the experimental results which then are discussed in Section 4.

1. Principles of the $(\Delta L/L_\circ - \Delta a/a_\circ)$ Method

The macroscopic volume V of a crystal can be expressed by the average volume of the atoms, Ω, and the number of atoms N in the crystal, i.e.

$$V = N\Omega . \tag{1}$$

A temperature change alters the volume of the crystal for various reasons. There is the normal thermal expansion due to anharmonic phonon interactions ΔV_{th}. If ΔN defects are created in thermal equilibrium a volume change $\Delta N \cdot \Delta v$ due to a lattice relaxation Δv around the defect occurs. Furthermore, in the case of Schottky defects, the volume changes due to the fact that for each thermally

created vacancy a new lattice site has to be created and occupied. This gives an additional volume change of one atomic volume Ω per vacancy. The total volume change is

$$\Delta V = \Delta V_{th} + \Delta N \cdot \Delta v + \Delta N \cdot \Omega . \tag{2}$$

Dividing (2) by $V_0 = N_0 \cdot \Omega_0$, the volume of the crystal at a reference temperature, gives

$$(\Delta V/V_0)_m = (\Delta V/V_0)_{th} + (\Delta N/N_0)(\Delta v/\Omega_0) + (\Delta N/N_0)(\Omega/\Omega_0) . \tag{3}$$

In general, the factor Ω/Ω_0 has been assumed unity. This is correct only in a first-order approximation. The mean atomic volume changes with temperature and due to lattice relaxation. The change of the average atomic volume $\Delta\Omega$ is measured by the X-ray lattice parameter change. The relative volume change as measured by X-rays is

$$(\Delta V/V_0)_X = \Delta\Omega/\Omega_0 = (\Delta V/V_0)_{th} + (\Delta N/N_0)(\Delta v/\Omega_0) . \tag{4}$$

Combination of (3) and (4) gives

$$\Delta N/N_0 = [(\Delta V/V_0)_m - (\Delta V/V_0)_X] \cdot (\Omega_0/\Omega) . \tag{5}$$

With (4) one gets

$$\Omega/\Omega_0 = (\Omega_0 + \Delta\Omega)/\Omega_0 = 1 + \Delta\Omega/\Omega_0 = 1 + (\Delta V/V_0)_X . \tag{6}$$

The macroscopic thermal expansion $(\Delta V/V_0)_m$ can be obtained from measurements of the sample dimensions. For a cubic crystal it suffices to measure the relative length change $\Delta L/L_0$, yielding

$$(\Delta V/V_0)_m = 3[\Delta L/L_0 + (\Delta L/L_0)^2 + (1/3)(\Delta L/L_0)^3] . \tag{7}$$

$(\Delta V/V_0)_X$ can be determined from the relative lattice parameter change $\Delta a/a_0$, i.e.

$$(\Delta V/V_0)_X = 3[\Delta a/a_0 + (\Delta a/a_0)^2 + (1/3)(\Delta a/a_0)^3] . \tag{8}$$

The quadratic terms have so far been neglected. They give a temperature dependent correction of the defect concentration up to 2%. Cubic terms may indeed be neglected.

Equations (7) and (8) give together with (5) and (6) the final result, in which cubic terms are neglected

$$\Delta N/N_0 = 3(\Delta L/L_0 - \Delta a/a_0)(1 + \Delta L/L_0 - 2\Delta a/a_0) . \tag{9}$$

Neglecting the second term in the right hand bracket gives the approximation commonly used. Taking for L_0 and a_0 the values at room temperature typical values for $\Delta L/L_0$ and $\Delta a/a_0$ close to the melting point are in the order of $2 \cdot 10^{-2}$.

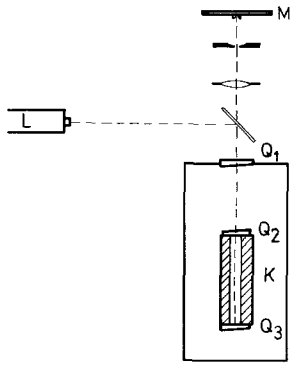

Fig. 1. Laser interferometer for the length change measurements

2. Experimental Procedure

We have measured the macroscopic length change by an interferometric method similar to that used by Feder and Charbnau [8]. This method allows to use smaller crystals (max. 5 cm) than for example Simmons and Balluffi [5] used in their measurements (50 cm). Using a smaller sample reduces the problem of having a constant temperature over the whole sample. The X-ray measurements were performed with a diffractometer on the same crystal simultaneously with the length measurements.

2.1. Length Change Measurements

Length change was measured with an interferometer using a He–Ne laser as a light source. The sample crystal had a central hole of 7 mm diameter parallel to its main axis (see Fig. 1). The sample rests upon an optical quartz flat Q_3 from which the laser beam is reflected. A second flat Q_2 rests on top of the sample. Between the two flats interferences due to equal thickness are produced and can be observed as fringes on the ground glass M. The optical flats Q_3 and Q_2 have faces of optical quality. The faces of each flat have a small angle of inclination to avoid reflections from the faces which do not touch the sample. The flats had dimensions of about $18 \times 18 \times 2\,mm^3$ and a weight of about 2 p.

The sample crystal is enclosed in the furnace. The laser beam enters the furnace through the window Q_1 which is another quartz flat as described above.

As the crystal expands with increasing temperature the optical path between Q_3 and Q_2 is changed, and

the fringe pattern moves across the ground glass. If z fringes pass a mark the length of the crystal has changed by

$$\Delta L = z\lambda_L/2\,, \tag{10}$$

where λ_L denotes the laser wavelength.
Due to a temperature change from room temperature to 630° C about 3000 fringes pass the mark. Therefore an automatic recording system was added. Two Si photo detectors (Siemens BPY 11, $4.8 \times 2.2 \times 0.8\,\text{mm}^3$) were mounted with 0.5 mm wide slits in front of the ground glass. The detectors were connected with a double pen strip chart recorder. The shift of the fringes is registered as a sine type curve. The photo detectors have been somewhat shifted in their position so that the two sine waves have a phase shift of $\pi/2$. This enables one to determine the direction of the fringe shift, and thus to obtain always the exact number of fringes. The relative length change is given by

$$\Delta L/L_0 = (z \cdot \lambda_L)/(2L_0)\,. \tag{11}$$

The crystal length L_0 at room temperature was determined by a micrometer caliper comparing it with length standards to $\pm 10^{-6}$ m. The He–Ne laser vacuum wave length $\lambda_L(\text{vac}) = 6328.142 \cdot 10^{-10}$ m was corrected for a 100 Torr He atmosphere in the furnace $\lambda_L(100\,\text{Torr He}) = 6328.114 \cdot 10^{-10}$ m.

2.2. Lattice Parameter Change Measurements

For the X-ray measurements a Hilger & Watts X-ray diffractometer was used. Figure 2 shows a schematic picture of the set-up. The front face of the sample K is adjusted to the center of the diffractometer circle DC. The X-ray tube XT with a Cu anode has the effective focus size $8 \times 0.04\,\text{mm}^2$. The X-ray beam is limited by slits and a Soller slit. Primary intensity is monitored by the scintillation counter Z_R. A small fraction of the X-ray beam is directed toward the monitor counter by a thin aluminum foil. The scintillation counter Z_A with an entrance slit detects the diffracted X-rays at an angle 2ϑ when the crystal is set at an angle ϑ. The scattered intensity distribution is determined in a $2\vartheta : \vartheta$ scan and I/I_0 is registered by a ratio strip chart recorder. Markings triggered by the diffractometer give the angle position on the chart. The relative lattice parameter change is derived from the shift $\Delta\vartheta = \vartheta - \vartheta_0$ of the diffraction peak using Bragg's law, i.e.

$$\Delta a = a - a_0 = (\lambda_{\text{Cu}}/2)\,(h^2 + k^2 + l^2)^{1/2} \cdot (1/\sin\vartheta - 1/\sin\vartheta_0)\,, \tag{12}$$

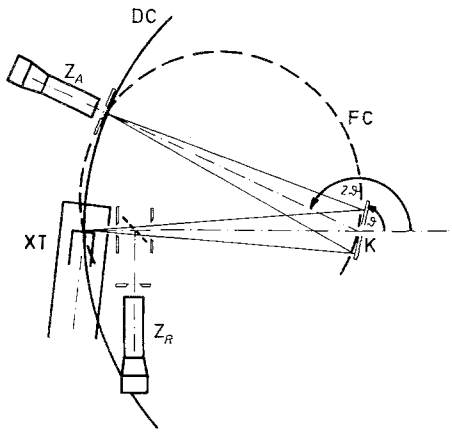

Fig. 2. X-ray diffractometer for the lattice parameter change measurements

where a_0 denotes the lattice parameter at room temperature, $\lambda_{\text{Cu}} = 1.54050 \cdot 10^{-10}$ m the X-ray wave length, (hkl) the Miller indices of the reflection planes.

2.3. Furnace

The furnace which allows the sample temperature to be controlled up to about 900° C is shown in Fig. 3. The sample *1* is surrounded by three heaters *2*, *3*, *4* which are controlled independently. Two NiCr–Ni thermocouples *5*, *6* measure the temperature difference between the top, bottom and center part of the sample, and give the input signal for the differential amplifiers of the heater current control [9, 10]. The sample temperature is measured by two additional NiCr–Ni thermocouples using a digital voltmeter with print out unit.
Two thin beryllium windows *7*, *8* allow the X-rays to enter and exit without strong attenuation.
The crystal holder rests on three insulating pins in such a manner that the front crystal face does not move due to thermal expansion. The chamber *9* is filled with 100 Torr He exchange gas to give better temperature homogeneity. Water with constant temperature flows through the double wall of *9*. Electrical feedthroughs *10* make the connections for the heatings and the thermocouples. The whole furnace rests with its bottom cone *11* on the corresponding cone of the diffractometer.

2.4. Specimen

A pure aluminum single crystal (99.999%) with dimensions $50 \times 20 \times 20\,\text{mm}^3$, purchased from the Metals Research Company, was used as a sample.

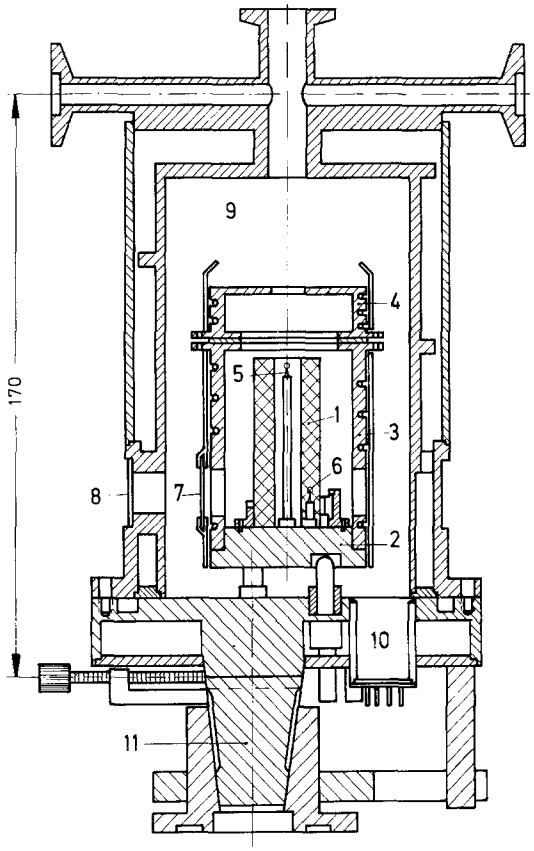

Fig. 3. High temperature furnace (explanation see text)

The crystal was oriented in [110] direction along its main dimension. The sample was spark cut from a single crystal bar so that the faces were (422) planes. The faces on which the optical flats rested were polished till they were parallel to each other to better than $5 \cdot 10^{-6}$ m. Small groves on these faces allowed exchange of the He gas into the central hole (7 mm diameter), which was spark drilled along the length axis. After the spark machining procedure the crystal was etched heavily and finally annealed at 900 K and cooled down slowly with about 10 deg/h to room temperature. The X-ray rocking curve showed that this Al single crystal was of mosaic type.

2.5. Precision of the Measurements

The error in the relative length change measurements comes mainly from the determination of the absolute length L_0 of the crystal. Minor errors come from the uncertainty of the laser wavelength, and the accuracy in counting interference fringes ($dz = 0.5$). This results in a maximum error of the relative length change measurements as follows:

for $400^\circ\,C < T < 640^\circ\,C$: $|d(\Delta L/L_0)| \leqq 7 \cdot 10^{-6}$,

for $T < 400^\circ\,C$: $|d(\Delta L/L_0)| \leqq 5 \cdot 10^{-6}$.

Relative lattice parameter changes could be measured with errors

for $300^\circ\,C < T < 640^\circ\,C$: $|d(\Delta a/a_0)| \leqq 3 \cdot 10^{-5}$,

for $T < 300^\circ\,C$: $|d(\Delta a/a_0)| \leqq 2.5 \cdot 10^{-5}$.

Although great care was taken to avoid a temperature gradient in the sample the major error comes from the temperature measurements and a possible temperature gradient. Measurements on a dummy with thermocouples fixed in holes in the crystal showed that the possibility of a temperature difference of up to 1 deg at 640° C over the whole sample length cannot be excluded. This can be described as an additional error in the lattice parameter change. Therefore the total error could be as high as:

for $T < 630^\circ\,C$: $|d(\Delta a/a_0)| \leqq 7 \cdot 10^{-5}$,

and $T < 300^\circ\,C$: $|d(\Delta a/a_0)| \leqq 5 \cdot 10^{-5}$.

2.6. General Remarks

The room temperature was kept constant at $(23 \pm 0.5)^\circ$ C. This is necessary for the optical set-up as well as for the diffractometer. During the experiment the crystal was warmed up at about 70 deg/h to the desired temperature. The X-ray measurement was performed at constant temperature and was started after the length of the crystal had no longer changed for 15 min. This was most sensitively monitored by the strip chart recorder which registers the interference fringes and gives a constant value after the crystal temperature has come to equilibrium. Holding the crystal at constant temperature for an extended period of time gave no changes. From this fact we conclude that the source and sink density in the crystal is high enough to establish the thermal equilibrium before the actual measurement.

3. Experimental Results

The interferometric method measures the length change ΔL. To obtain the relative length change one has to determine the length L_0 of the crystal at room temperature with high enough precision. The length of our sample at 21° C was $L_0 = (49.170 \pm 0.005)$ mm. Measurements before and after heating up during the experiment agreed within the error width. Since

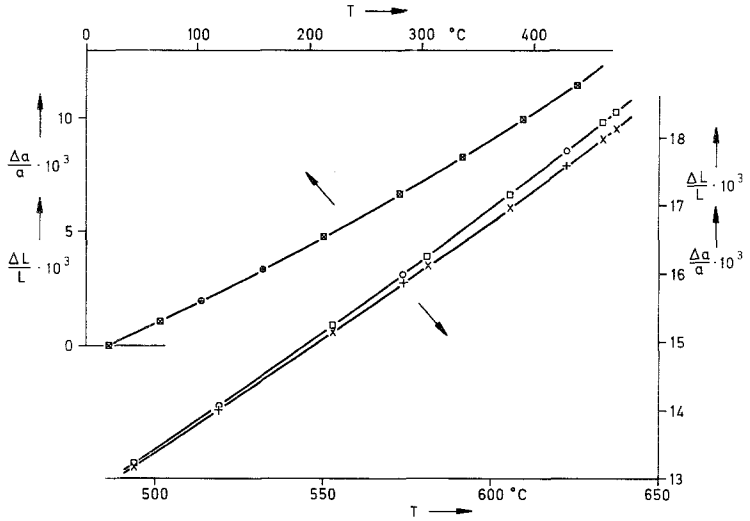

Fig. 4. Relative length change $\Delta L/L_0$ and relative lattice parameter change $\Delta a/a_0$ of aluminum versus temperature (□ $\Delta L/L_0$, × $\Delta a/a_0$ heating run and ○ $\Delta L/L_0$, + $\Delta a/a_0$ cooling run). Note the expanded scales above 500° C, to display the small differences between $\Delta L/L_0$ and $\Delta a/a_0$

an absolute determination of the X-ray lattice parameter is very difficult, a_0 was determined by the following procedure. At moderate temperatures (<200° C) the vacancy concentration is unmeasurable small. In this region $\Delta a/a_0 = \Delta L/L_0$ should hold at all temperatures. A least-square fit gave $a_0 = (4.05109 \pm 0.00003) \cdot 10^{-10}$ m. The stated error is the mean standard deviation of the fit. The value of a_0 is rather close to the value given in the literature ($a_0 = 4.0493$ Å [11]). It was used without further corrections.

Figure 4 shows values of $\Delta L/L_0$ and $\Delta a/a_0$ for the temperature range from room temperature to 640° C. Squares and Xes represent data measured during heating up, and circles and crosses during cooling down again. In the whole temperature range no hysteresis could be observed. For clarity only some characteristic data are indicated. In order to check whether values at certain temperatures are equal at heating and cooling several measurements were performed at the same or almost the same temperature. All data measured are given in the table in the Appendix. Up to almost 500° C $\Delta L/L_0$ and $\Delta a/a_0$ coincide. At higher temperatures $\Delta L/L_0$ becomes greater than $\Delta a/a_0$. Note the change in scale in the part of the figure for $T < 500°$ C! The full lines are computer fits to the experimental data points. The following polynomials of fifth order gave a satisfactory fit (t = temperature in °C):

$$\Delta a/a_0 = -0.513 \cdot 10^{-3} + 0.237 \cdot 10^{-4} t - 0.527 \cdot 10^{-8} t^2 + 0.674 \cdot 10^{-10} t^3 - 0.117 \cdot 10^{-12} t^4 + 0.711 \cdot 10^{-16} t^5,$$

$$\Delta L/L_0 = -0.509 \cdot 10^{-3} + 0.237 \cdot 10^{-4} t - 0.497 \cdot 10^{-8} t^2 + 0.705 \cdot 10^{-10} t^3 - 0.132 \cdot 10^{-12} t^4 + 0.885 \cdot 10^{-16} t^5.$$

4. Discussion

From Fig. 4 it can be seen that from about 500° C upwards $\Delta N/N_0$ increases. The positive value of $\Delta N/N_0$ indicates that the predominant defect is of vacancy type. The concentration of thermally created lattice sites at the melting point (660° C) is

$$\Delta N/N_0 = 9.8 \cdot 10^{-4}.$$

If C_{1V} monovacancies and C_{2V} divacancies are present in thermal equilibrium $\Delta N/N_0$ will have the following temperature dependence

$$\Delta N/N_0 = C_{1V} + 2C_{2V} = \exp(S^F_{1V}/k)\exp(-H^F_{1V}/kT) + 12\exp(S^F_{2V}/k)\exp(-H^F_{2V}/kT), \quad (15)$$

where S^F_{1V}, S^F_{2V} and H^F_{1V}, H^F_{2V} are the entropy and enthalpy of formation, respectively, of monovacancies and divacancies. The following relations between monovacancy and divacancy parameters are usually introduced

$$S^F_{2V} = 2S^F_{1V} + \Delta S_{2V} \qquad H^F_{2V} = 2H^F_{1V} - E^B_{2V}, \quad (17)$$

where E^F_{2V} is the divacancy binding energy, and ΔS_{2V} the change in the non configurational part of the entropy due to divacancy formation. Figure 5 shows the temperature dependence of $\Delta N/N_0$ in the usual semilog $1/T$ plot. $\Delta N/N_0$ values were calculated according to (9) using the smoothed values of the computer fit of $\Delta L/L_0$ and $\Delta a/a_0$, respectively (full circles). Only $\Delta N/N_0 > 10^{-4}$ are plotted and were used in the following evaluation.

In Fig. 5 values obtained by Simmons and Balluffi [5] (triangles) and by Bianchi *et al.* [6] (squares) are

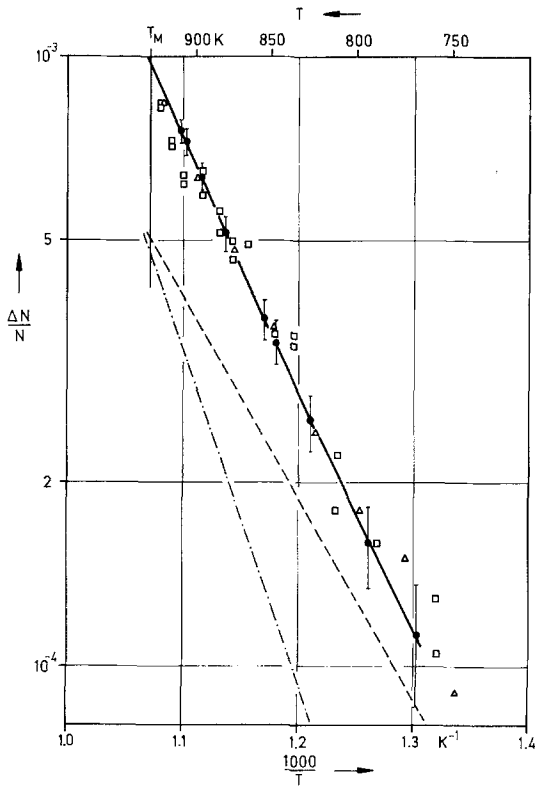

Fig. 5. Semi-logarithmic plot of the equilibrium vacancy concentration versus reciprocal temperature (● present results with standard deviation, ——— $C_{1V} = 1.82 \exp(-0.66\ \mathrm{eV}/kT)$, –·–·– $2C_{2V} = 359.56 \exp(-1.09\ \mathrm{eV}/kT)$, △ Simmons and Balluffi [5], □ Bianchi *et al.* [6])

also given for comparison. The latter two sets of data have not been corrected for the quadratic terms in (9). Such a correction would lower these data points by a maximum of 2%. Within the given error width all three sets of data agree very well.

Since the data points show only little deviation from laying on a straight line, as a first attempt an effective formation enthalpy and entropy can be determined in a two parameter fit

$$\Delta N/N_0 = \exp(S_{\mathrm{eff}}/k) \exp(-H_{\mathrm{eff}}/kT) . \tag{16}$$

The effective values for vacancy formation are then

$$S_{\mathrm{eff}} = 3.12\,k \quad \text{and} \quad H_{\mathrm{eff}} = 0.81\ \mathrm{eV} .$$

As a second attempt to interpret our data we have taken the value for the monovacancy formation enthalpy $H^F_{1V} = 0.66$ eV determined from positron annihilation experiments and made a three parameter fit according (16). In Fig. 5 the solid line represents the result of this fit given by

$$\Delta N/N = 1.82 \exp(-0.66\ \mathrm{eV}/kT) + 359.56 \exp(-1.09\ \mathrm{eV}/kT) . \tag{17}$$

The following monovacancy and divacancy parameters would be consistent with our measurements.

$$H^F_{1V} = 0.66\ \mathrm{eV}, \quad S^F_{1V} = 0.6\,k,$$
$$S_{2V} = 2.2\,k, \quad E^B_{2V} = 0.23\ \mathrm{eV} .$$

The dashed line in Fig. 5 gives the monovacancy concentration C_{1V} [first part of (17)] and the dash-dotted line gives the divacancy concentration $2C_{2V}$. At the melting point $2C_{2V}/(C_{1V} + 2C_{2V}) \approx 50\%$. Unfortunately it is not possible with our present accuracy to decide unambiguously which fit is correct.

Acknowledgement. The authors wish to thank Prof. W. Waidelich for his current interest in this work. Many thanks are due to K. Wandel and W. Poth for their assistance. One of us (H.P.) is very much indebted to Prof. R. O. Simmons for many stimulating discussions and critical comments. Special thanks are due to Prof. A. Seeger for clarifying discussions and critically reading the manuscript, and Dr. H. Mehrer who assisted us in the computer evaluation of the results.

Appendix

Table 1. Summary of data

$(\Delta a/a_0)_{\mathrm{exp}}$	experimental lattice parameter change
$(\Delta a/a_0)_{\mathrm{fit}}$	data from the fit curve of all $(\Delta a/a_0)_{\mathrm{exp}}$ by a polynome
$(\Delta L/L_0)_{\mathrm{exp}}$	experimental length change
$(\Delta L/L_0)_{\mathrm{fit}}$	data from the fit curve of all $(\Delta L/L_0)_{\mathrm{exp}}$ by a polynome

T[°C]	$(\Delta a/a_0)_{\mathrm{exp}}$	$(\Delta a/a_0)_{\mathrm{fit}}$	$(\Delta L/L_0)_{\mathrm{exp}}$	$(\Delta L/L_0)_{\mathrm{fit}}$
Measurements during heating up				
21.83	0.00003	0.00000	0.00000	0.00000
40.85	0.00048	0.00045	0.00047	0.00045
66.66	0.00111	0.00106	0.00108	0.00106
104.92	0.00201	0.00198	0.00199	0.00199
156.75	0.00329	0.00327	0.00328	0.00328
213.27	0.00482	0.00475	0.00483	0.00476
281.06	0.00646	0.00663	0.00652	0.00665
336.93	0.00832	0.00827	0.00836	0.00828
391.59	0.00998	0.00993	0.01000	0.00994
438.73	0.01142	0.01140	0.01146	0.01142
494.07	0.01321	0.01318	0.01324	0.01322
552.91	0.01516	0.01514	0.01521	0.01523
553.20	0.01518	0.01515	0.01527	0.01524
581.36	0.01615	0.01612	0.01629	0.01624
605.95	0.01699	0.01698	0.01717	0.01716
633.57	0.01799	0.01798	0.01829	0.01822
637.46	0.01808	0.01812	0.01834	0.01838
Measurements during cooling down				
622.74	0.01757	0.01758	0.01774	0.01780
574.21	0.01586	0.01587	0.01595	0.01599

(Continued)

T [°C]	$(\Delta a/a_0)_{exp}$	$(\Delta a/a_0)_{fit}$	$(\Delta L/L_0)_{exp}$	$(\Delta L/L_0)_{fit}$
519.54	0.01395	0.01402	0.01403	0.01408
467.69	0.01229	0.01233	0.01234	0.01236
467.02	0.01226	0.01231	0.01233	0.01233
413.68	0.01058	0.01061	0.01059	0.01063
361.50	0.00905	0.00901	0.00898	0.00902
303.95	0.00734	0.00729	0.00729	0.00731
226.61	0.00511	0.00511	0.00517	0.00512
158.23	0.00326	0.00331	0.00327	0.00331
104.10	0.00194	0.00196	0.00194	0.00197
68.95	0.00111	0.00112	0.00112	0.00112
44.77	0.00053	0.00054	0.00055	0.00055
21.71	−0.00005	0.00000	−0.00000	0.00000

References

1. A. Seeger: J. Phys. F (Metal Phys.) **3**, 248 (1973)
2. A. Seeger: *Crystal Lattice Defects*, to be published
3. A. Seeger, H. Mehrer: In *Vacancies and Interstitials in Metals*, ed. by Seeger, Schumacher, Schilling and Diehl (North Holland Publishing Comp., Amsterdam 1969) p. 42
4. R. Feder, A. S. Nowick: Phys. Rev. **109**, 1959 (1958)
5. R. O. Simmons, R. W. Balluffi: Phys. Rev. **117**, 52 (1960)
6. G. Bianchi, D. Mallejac, C. Janot, G. Champier: Compt. Rend. Acad. Sci. (Paris) B **263**, 1404 (1966)
7. B. T. A. McKee, W. Triftshäuser, A. T. Stewart: Phys. Rev. Letters **28**, 358 (1972)
8. R. Feder, H. P. Charbnau: Phys. Rev. **149**, 464 (1966)
9. H. Behrendt: Diplomarbeit, TH Darmstadt 1970
10. K. Wandel: Diplomarbeit, TH Darmstadt 1972
11. A. J. Cornish, J. Burke: J. Sci. Instr. **42**, 212 (1965)